

Extracting nucleon strange and anapole form factors from world data

R. D. Young¹, J. Roche, R. D. Carlini¹, and A. W. Thomas¹
¹*Jefferson Lab, 12000 Jefferson Ave., Newport News, VA 23606 USA*

Using the complete world set of parity violating electron scattering data up to $Q^2 \sim 0.3 \text{ GeV}^2$, we extract the current best determination of the strange electric and magnetic form factors of the proton, as well as the weak axial form factors of the proton and neutron at $Q^2 = 0.1 \text{ GeV}^2$. The results are consistent with state of the art calculations of all four form factors, with the latter including the anapole contribution.

PACS numbers: 13.60.-r 11.30.Er 14.20.Dh 25.30.Bf

Parity-violating electron scattering (PVES) is an essential tool in mapping out the flavor composition of the electromagnetic form factors. Exposing the role of the strange quark via these measurements provides direct information on the underlying dynamics of nonperturbative QCD — a compelling achievement both experimentally and theoretically. The most precise separation of the strange electric and magnetic form factors is available at $Q^2 \simeq 0.1 \text{ GeV}^2$, where experiments by the SAMPLE [1, 2], PVA4 [3] and HAPPEX [4, 5] collaborations have been performed with varying kinematics and targets. At higher Q^2 , HAPPEX [6, 7], PVA4 [8] and the forward angle G0 experiment [9] provide further information over the range $Q^2 \sim 0.12\text{--}1.0 \text{ GeV}^2$. Here we use systematic expansions of all the unknown form factors to simultaneously analyze the current data set and extract the values at $Q^2 = 0.1 \text{ GeV}^2$, independent of theoretical input — other than the constraint of charge symmetry. The results provide a critical test of modern theoretical estimates of the anapole moment of the proton and neutron as well as their strange form factors.

The proton-PVES experiments are sensitive to the strange form factors G_E^s and G_M^s , and the electroweak axial form factor \tilde{G}_A^p — which is subject to significant QCD radiative corrections [10, 11]. Previously, limited experimental data made it difficult to carry out a simultaneous separation of all three form factors; instead, assumptions were made on the (in)significance of certain contributions based on the kinematic domain and/or the use of theoretical calculations. For example: The SAMPLE analysis [2] used theoretical estimates [11] for the nonperturbative QCD corrections to the axial form factor in their extraction of the strange form factors. The effect of this was to reduce the error quoted for the strange magnetic form factor. However, the ultimate goal is to determine both the vector and axial form factors from experimental data without theoretical input on any form factor. The current global data set is now extensive enough to permit us to make such an analysis.

The role of the strange quark is probed by measuring the PV asymmetry in $e\text{-}p$ scattering, for which the dominant piece arises from interference between the γ and Z^0 exchange. The majority of measurements have been performed on hydrogen: SAMPLE [2, 12], HAPPEX [5, 6],

PVA4 [3, 8] and G0 [9]. All of these experiments, except SAMPLE, measured scattering at forward angles, where the contribution from the axial form factor is suppressed. Such experiments are particularly sensitive to a linear combination of the two strange vector form factors.

As described in Ref. [13], the PV asymmetry for a proton target is given by (assuming charge symmetry)

$$A_{LR}^p = \frac{d\sigma_R - d\sigma_L}{d\sigma_R + d\sigma_L} = -\frac{G_\mu Q^2}{4\pi\alpha\sqrt{2}} \frac{A_V^p + A_s^p + A_A^p}{\epsilon G_E^{p,2} + \tau G_M^{p,2}}, \quad (1)$$

$$A_V^p = \xi_V^p (\epsilon G_E^{p,2} + \tau G_M^{p,2}) + \xi_V^n (\epsilon G_E^p G_E^n + \tau G_M^p G_M^n), \quad (2)$$

$$A_s^p = \epsilon G_E^p \xi_V^0 G_E^s + \tau G_M^p \xi_V^0 G_M^s, \quad (3)$$

$$A_A^p = -(1 - 4\hat{s}^2) \sqrt{1 - \epsilon^2} \sqrt{\tau(1 + \tau)} G_M^p \tilde{G}_A^p. \quad (4)$$

The kinematic variables are defined by $\epsilon \equiv [1 + 2(1 + \tau) \tan^2 \theta/2]^{-1}$ and $\tau \equiv |Q^2|/4M_p^2$. The Standard Model parameters α , G_μ and $\hat{s}^2 \equiv \sin^2 \hat{\theta}_W$ are taken from the PDG [14]. The vector radiative correction factors are defined by $\xi_V^p = (1 - 4\hat{s}^2)(1 + R_V^p)$, $\xi_V^n = -(1 + R_V^n)$ and $\xi_V^0 = -(1 + R_V^{(0)})$, with $R_V^p = -0.04471$ and $R_V^n = R_V^{(0)} = -0.01179$ [14]. The axial radiative and anapole corrections remain implicit in \tilde{G}_A^p , as this entire contribution is to be fit to data.

Scattering from targets other than the proton provides access to different flavour components of the nucleon form factors. The HAPPEX Collaboration have recently utilised a helium-4 target to directly extract the strange electric form factor [4], where the theoretical asymmetry can be written as

$$A_{LR}^{\text{He}} = -\frac{G_\mu Q^2}{4\pi\alpha\sqrt{2}} \left[(\xi_V^p + \xi_V^n) - 2 \frac{\xi_V^0 G_E^s}{G_E^p + G_E^n} \right]. \quad (5)$$

In the SAMPLE experiment, which detected electrons scattered at backward angles, the contribution from G_E^s is significantly suppressed. These measurements were thereby sensitive primarily to a linear combination of the axial and strange magnetic form factors. In addition to the proton target, the PV-asymmetry has also been measured on the deuteron [1]. While providing a different combination of G_M^s and \tilde{G}_A^p , this also introduces sensitivity to the neutron axial form factor.

TABLE I: Displayed are the η_i , appearing in Eq. (6), which describe the theoretical asymmetry for each experiment. The measured asymmetry is shown by A^{phys} and the corresponding uncertainty, δA , where sources of error have been added in quadrature. The second uncertainty, δA_{cor} , represents the correlated error in the G0 experiment [9]. Columns on the right show the determination of the form factors at $Q^2 = 0.1 \text{ GeV}^2$ for fits which include all data up to the given measurement (statistical uncertainty only). The reduced χ^2 for each fit is displayed in the final column.

Collaboration	Q^2	η_0	η_A^p	η_A^n	η_E	η_M	A^{phys}	δA	δA_{cor}	\tilde{G}_A^p	\tilde{G}_A^n	G_E^s	G_M^s	χ^2
SAMPLE	0.038	-2.13	0.46	-0.30	1.16	0.28	-3.51	0.81	0	—	—	—	—	—
SAMPLE	0.091	-7.02	1.04	-0.65	1.63	0.77	-7.77	1.03	0	—	—	—	—	—
HAPPEX	0.091	-7.50	0	0	-20.2	0	-6.72	0.87	0	—	—	—	—	—
HAPPEX	0.099	-1.40	0.04	0	9.55	0.76	-1.14	0.25	0	—	—	—	—	—
SAMPLE	0.1	-5.47	1.58	0	2.11	3.46	-5.61	1.11	0	-2.6(21)	-0.6(30)	-0.044(47)	1.00(75)	1.0
PVA4	0.108	-1.80	0.26	0	10.1	1.05	-1.36	0.32	0	-2.0(20)	0.3(29)	-0.025(43)	0.87(74)	1.0
G0	0.122	-1.90	0.06	0	12.0	1.18	-1.51	0.49	0.18	-1.8(19)	0.5(27)	-0.023(43)	0.79(69)	0.7
G0	0.128	-2.04	0.06	0	12.6	1.30	-0.97	0.46	0.17	-2.4(18)	-0.1(26)	-0.027(42)	0.99(65)	0.7
G0	0.136	-2.24	0.07	0	13.5	1.48	-1.30	0.45	0.17	-2.5(17)	-0.2(26)	-0.028(42)	1.03(63)	0.6
G0	0.144	-2.44	0.08	0	14.3	1.67	-2.71	0.47	0.18	-1.6(16)	0.8(25)	-0.021(42)	0.71(61)	1.4
G0	0.153	-2.68	0.09	0	15.3	1.89	-2.22	0.51	0.21	-1.4(16)	1.0(25)	-0.020(42)	0.66(60)	1.2
G0	0.164	-2.97	0.11	0	16.5	2.19	-2.88	0.54	0.23	-1.1(16)	1.3(25)	-0.018(42)	0.55(60)	1.2
G0	0.177	-3.34	0.13	0	18.0	2.58	-3.95	0.50	0.20	-0.4(16)	2.1(24)	-0.012(42)	0.32(59)	1.7
G0	0.192	-3.78	0.15	0	19.7	3.07	-3.85	0.53	0.19	-0.2(15)	2.3(24)	-0.010(42)	0.24(58)	1.6
G0	0.210	-4.34	0.19	0	21.8	3.72	-4.68	0.54	0.21	0.1(15)	2.7(24)	-0.007(42)	0.14(57)	1.6
PVA4	0.230	-5.66	0.89	0	22.6	5.07	-5.44	0.60	0	0.0(15)	2.5(24)	-0.007(42)	0.14(57)	1.5
G0	0.232	-5.07	0.23	0	24.4	4.61	-5.27	0.59	0.23	0.2(14)	2.8(23)	-0.005(42)	0.09(57)	1.4
G0	0.262	-6.12	0.31	0	28.0	5.99	-5.26	0.53	0.17	-0.2(14)	2.3(23)	-0.010(41)	0.19(56)	1.4
G0	0.299	-7.51	0.42	0	32.6	8.00	-7.72	0.80	0.35	0.0(14)	2.6(23)	-0.006(41)	0.12(55)	1.3
G0	0.344	-9.35	0.57	0	38.4	10.9	-8.40	1.09	0.52	0.0(14)	2.5(22)	-0.008(41)	0.15(54)	1.2
G0	0.410	-12.28	0.87	0	47.3	16.1	-10.25	1.11	0.55	-0.4(13)	2.1(22)	-0.015(40)	0.27(53)	1.2
HAPPEX	0.477	-15.46	1.12	0	56.9	22.6	-15.05	1.13	0	0.1(12)	2.7(21)	-0.004(38)	0.10(49)	1.2

Scattering from the deuteron is dominated by the quasielastic interaction with the nucleon constituents. The analysis of the deuteron results [12] has also included nuclear corrections, involving a realistic deuteron wavefunction, rescattering effects and the small contribution from elastic deuteron scattering [15]. Further parity-violating contributions arising from the deuteron wavefunction and exchange currents, while small [15], have been included.

A combined analysis of the current world PV data requires a consistent treatment of the vector and axial form factors and radiative corrections. Our theoretical asymmetries have therefore been reconstructed for each measurement, including the nuclear corrections in the case of the deuteron target. The theoretical asymmetry, in parts-per-million, is described by

$$A_{PV}^{theory} = \eta_0 + \eta_A^p \tilde{G}_A^p + \eta_A^n \tilde{G}_A^n + \eta_E G_E^s + \eta_M G_M^s, \quad (6)$$

where the values of η_i , which are given in Table I, include the latest electromagnetic form factors [16] and PDG radiative corrections.

It has been observed that the strange form factors are mildly sensitive to the choice of form factor parameterisation, with an uncertainty dominated by the neutron charge form factor. To test the sensitivity to G_E^n , we explicitly included the experimental data for G_E^n [17] in our global fit. Over the low- Q^2 domain required in this

analysis, the form factor can be parameterised by a Taylor expansion up to $\mathcal{O}(Q^6)$. This made no significant difference to the final extraction, and hence the central value of the Kelly parameterisation [16] is taken in the following analysis.

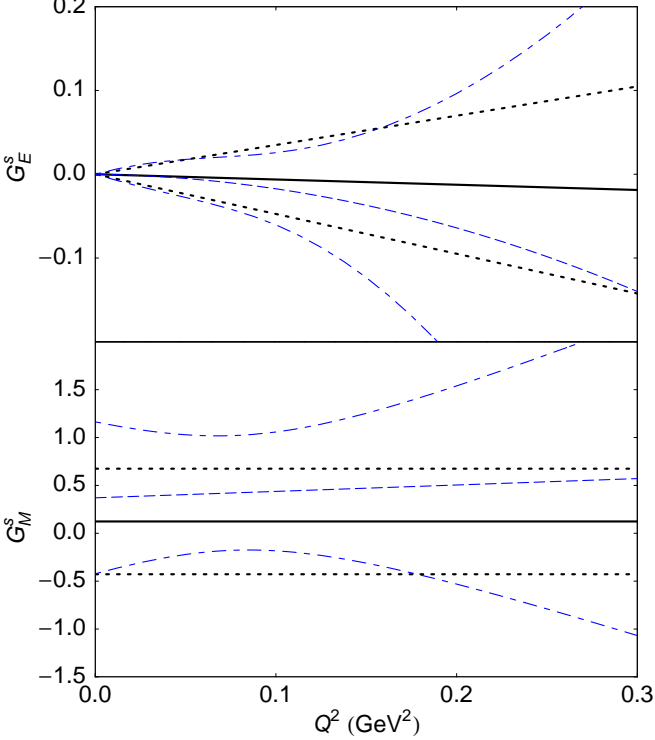
In order to extract all three form factors using as much data as possible, we parameterise their Q^2 dependence. At low momentum transfer, a Taylor series expansion in Q^2 is sufficient and minimises the model-dependence of the determined form factors. The quality of a Taylor series expansion can be estimated phenomenologically. Vector meson dominance would suggest that the Q^2 evolution of the form factors be no more rapid than a dipole with mass parameter $\sim m_\phi \sim 1 \text{ GeV}$. Similarly, lattice QCD simulations in the vicinity of the strange quark yield behaviour consistent with a dipole of scale $> 1 \text{ GeV}$ [18, 19]. With the aim of fitting data up to $Q^2 \sim 0.3 \text{ GeV}^2$, approximating a dipole by a constant over this range would lead to less than 20% uncertainty (less than 10% at the next order in Q^2).

To isolate the individual form factors beyond this low-energy range, a combination of neutrino and parity-violating electron scattering should provide the tightest constraint, as described in Ref. [20].

We describe the Q^2 -dependence of the form factors over the range $0 < Q^2 < 0.3 \text{ GeV}^2$ by

$$\tilde{G}_A^N = \tilde{g}_A^N (1 + Q^2/M_A^2)^{-2} \quad (7)$$

FIG. 1: The strange electric and magnetic form factors. The solid curve shows the leading-order fit, with $1-\sigma$ bound shown by the dotted curves. The dashed and dash-dotted curves show the fit and error of the next-to-leading order fit.



$$G_E^s = \rho_s Q^2 + \rho'_s Q^4 \quad (8)$$

$$G_M^s = \mu_s + \mu'_s Q^2 \quad (9)$$

The momentum dependence of the radiative corrections are assumed to be mild, and therefore the axial dipole mass is chosen to be that determined from neutrino scattering, $M_A = 1.026 \text{ GeV}$ [21].

The best fit for $Q^2 < 0.3 \text{ GeV}^2$ yields, at leading-order in Q^2 , a reduced $\chi^2 = 19.7/15 = 1.3$, with parameters

$$\tilde{g}_A^p = 0.05 \pm 1.38 \mp 0.29, \quad (10)$$

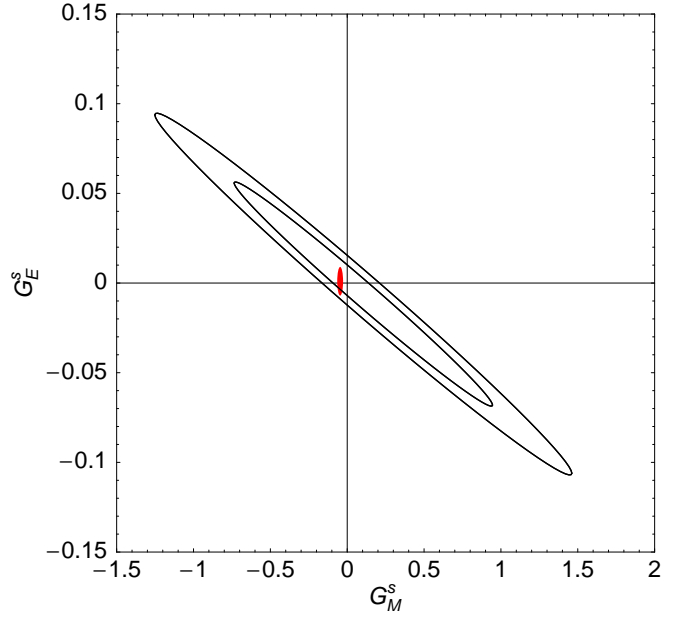
$$\tilde{g}_A^n = 2.61 \pm 2.27 \mp 0.37, \quad (11)$$

$$\rho_s = -0.06 \pm 0.41 \mp 0.00 \text{ GeV}^{-2}, \quad (12)$$

$$\mu_s = 0.12 \pm 0.55 \pm 0.07. \quad (13)$$

The second error bar displays the sensitivity of the fits to the correlated background subtraction in the G0 experiment, where the data has been refit using $A^{phys} \pm \delta A_{cor}$. These resultant extraction of the strange form factors over the low- Q^2 range is shown in Fig. 1. We display the joint determination of the strange electric and magnetic form factors at $Q^2 = 0.1 \text{ GeV}^2$ in Fig. 2, where we compare the theoretical calculations of Leinweber et al. [22, 23]. Similar contours in $\tilde{G}_A^p - G_M^s$ and $\tilde{G}_A^p - \tilde{G}_A^n$ space are shown in Fig. 3.

FIG. 2: The contours display the the 68 and 95% confidence intervals for the joint determination of G_M^s and G_E^s at $Q^2 = 0.1 \text{ GeV}^2$. The solid ellipse depicts the theory result [22, 23].



The sensitivity of the upper Q^2 range has been investigated, where the fits are found to stabilise in the vicinity of $Q^2 \sim 0.2 \text{ GeV}^2$. The determined form factors, evaluated at $Q^2 = 0.1 \text{ GeV}^2$, are shown for each fit in Table I.

Including the next order term in the expansion of the strange form factors produces a $\chi^2 = 18.1/13 = 1.4$ and best-fit parameters $\tilde{g}_A^p = -0.80 \pm 1.68$, $\tilde{g}_A^n = 1.65 \pm 2.62$, $\rho_s = -0.03 \pm 0.63 \text{ GeV}^{-2}$, $\rho'_s = -1.5 \pm 5.8 \text{ GeV}^{-4}$, $\mu_s = 0.37 \pm 0.79$ and $\mu'_s = 0.7 \pm 6.8 \text{ GeV}^{-2}$, where errors are statistical only. There is no statistical support for these terms based on the present data, and results are clearly consistent with the leading result, as shown in Fig. 1.

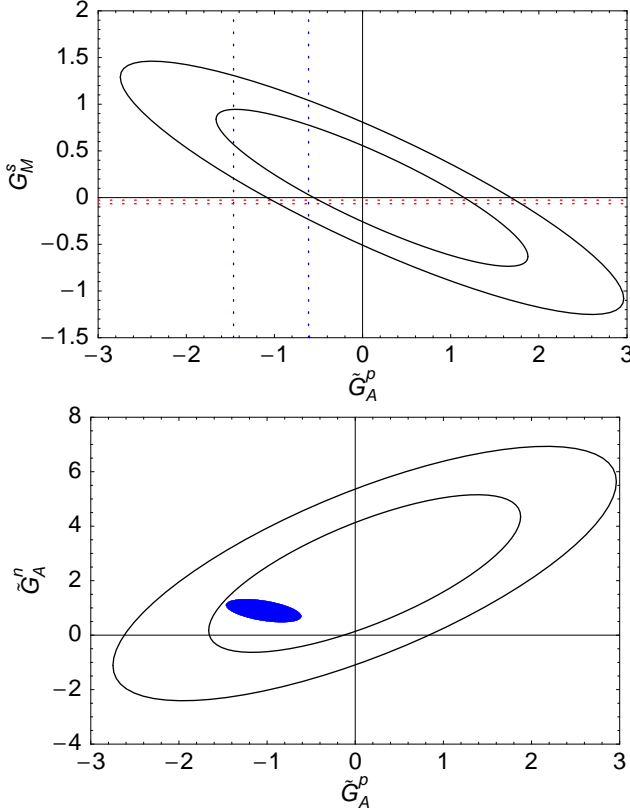
To compare with the anapole contributions reported by Zhu et al. [11], it is convenient to decompose the axial form factors into isovector and isoscalar components,

$$\tilde{G}_A^N = \xi_A^{T=1} G_A \tau_3 + \xi_A^{T=0} a_8 + \xi_A^0 a_s + A_{ana}^N, \quad (14)$$

with $\tau_3 = 1(-1)$ for proton (neutron). The radiative corrections are implied to be single-quark only $\xi_A^{T=1} = -0.828$, $\xi_A^{T=0} = -0.126$ and $\xi_A^0 = 0.449$ [14]. The multi-quark or anapole terms are explicitly contained in $A_{ana}^N = A_{ana}^{(T=1)} \tau_3 + A_{ana}^{(T=0)}$. Taking their estimates and converting the results to \overline{MS} [24], the anapole terms are estimated to be $A_{ana}^{(T=1)} = -0.11 \pm 0.44$ and $A_{ana}^{(T=0)} = 0.02 \pm 0.26$.

For estimates of the axial charges, we use $G_A = 1.2695$, $a_8 = 0.58 \pm 0.03 \pm 0.12$ [25] and $a_s = -0.07 \pm 0.04 \mp 0.05$ [26]. The second error in a_8 and a_s reflects estimates of the SU(3)-flavour symmetry violations of 20% in the determination of a_8 from hyperon β -decay [27]. This gives

FIG. 3: The contours display the the 68 and 95% confidence intervals for the joint determination of the form factors (defined on the axes) at $Q^2 = 0.1 \text{ GeV}^2$. The horizontal band in the upper panel shows the Leinweber et al. [22] result for μ_s and the vertical band based on the anapole calculation of Zhu et al. [11]. The disk in the lower panel displays the theoretical result of Zhu et al. [11], assuming the same dipole behaviour as Eq. (7).



the total estimates for the axial charges in PVES

$$\tilde{G}_A^p = (-1.16 \pm 0.04) + (-0.09 \pm 0.51), \quad (15)$$

$$\tilde{G}_A^n = (0.95 \pm 0.04) + (0.13 \pm 0.51), \quad (16)$$

where the second term is the anapole contribution. These estimates are compared with the present determination in the lower panel of Fig. 3. The upper panel of this figure makes it evident that constraining to the anapole estimates of Zhu et al. [11] suggests a positive value for the strange magnetic form factor, but no such conclusion can be drawn from experimental data alone.

In conclusion, our analysis of the world data set for PVES has yielded the best experimental determination, at low Q^2 , of the strange electric and magnetic form factors of the proton as well as the axial form factors of the proton and neutron, including hadronic radiative corrections. All four form factors are in agreement with the best theoretical estimates but with relatively large errors. We expect that the present HAPPEX and G0-

backward angle experiments at Jefferson Lab and the PVA4-backward angle experiment at Mainz will soon yield data that, when combined with this analysis, will improve this situation dramatically.

We wish to express our gratitude to M. Pitt, D. Bowman, K. de Jager, W. Melnitchouk, M. Paris, K. Paschke and R. Schiavilla for helpful discussions. This work was supported by DOE contract DE-AC05-84ER40150, under which SURA operates Jefferson Lab.

[1] T. M. Ito *et al.* [SAMPLE Collaboration], Phys. Rev. Lett. **92**, 102003 (2004) [arXiv:nucl-ex/0310001].
[2] D. T. Spayde *et al.* [SAMPLE Collaboration], Phys. Lett. B **583**, 79 (2004) [arXiv:nucl-ex/0312016].
[3] F. E. Maas *et al.*, Phys. Rev. Lett. **94**, 152001 (2005).
[4] K. A. Aniol *et al.* [HAPPEX Collaboration], Phys. Rev. Lett. **96**, 022003 (2006) [arXiv:nucl-ex/0506010].
[5] K. A. Aniol *et al.* [HAPPEX Collaboration], Phys. Lett. B **635**, 275 (2006) [arXiv:nucl-ex/0506011].
[6] K. A. Aniol *et al.* [HAPPEX Collaboration], Phys. Lett. B **509**, 211 (2001) [arXiv:nucl-ex/0006002].
[7] K. A. Aniol *et al.* [HAPPEX Collaboration], Phys. Rev. C **69**, 065501 (2004) [arXiv:nucl-ex/0402004].
[8] F. E. Maas *et al.* [A4 Collaboration], Phys. Rev. Lett. **93**, 022002 (2004) [arXiv:nucl-ex/0401019].
[9] D. S. Armstrong *et al.* [G0 Collaboration], Phys. Rev. Lett. **95**, 092001 (2005) [arXiv:nucl-ex/0506021].
[10] M. J. Musolf and B. R. Holstein, Phys. Lett. B **242**, 461 (1990).
[11] S. L. Zhu *et al.*, Phys. Rev. D **62**, 033008 (2000).
[12] E. J. Beise, M. L. Pitt and D. T. Spayde, Prog. Part. Nucl. Phys. **54**, 289 (2005) [arXiv:nucl-ex/0412054].
[13] M. J. Musolf *et al.*, Phys. Rept. **239**, 1 (1994).
[14] S. Eidelman *et al.* [PDG], Phys. Lett. B **592**, 1 (2004).
[15] R. Schiavilla *et al.*, Phys. Rev. C **70**, 044007 (2004).
R. Schiavilla *et al.*, Phys. Rev. C **67**, 032501 (2003).
[16] J. J. Kelly, Phys. Rev. C **70**, 068202 (2004).
[17] C. E. Hyde-Wright and K. de Jager, Ann. Rev. Nucl. Part. Sci. **54**, 217 (2004) [arXiv:nucl-ex/0507001].
[18] M. Gockeler *et al.* [QCDSF Collaboration], Phys. Rev. D **71**, 034508 (2005) [arXiv:hep-lat/0303019].
[19] J. D. Ashley *et al.*, Eur. Phys. J. A **19**, 9 (2004) [arXiv:hep-lat/0308024].
[20] S. F. Pate, Phys. Rev. Lett. **92**, 082002 (2004) [arXiv:hep-ex/0310052].
[21] V. Bernard, L. Elouadrhiri and U. G. Meissner, J. Phys. G **28**, R1 (2002) [arXiv:hep-ph/0107088].
[22] D. B. Leinweber *et al.*, Phys. Rev. Lett. **94**, 212001 (2005) [arXiv:hep-lat/0406002].
[23] D. B. Leinweber *et al.*, arXiv:hep-lat/0601025.
[24] K. S. Kumar and P. A. Souder, Prog. Part. Nucl. Phys. **45**, S333 (2000).
[25] B. W. Filippone and X. D. Ji, Adv. Nucl. Phys. **26**, 1 (2001) [arXiv:hep-ph/0101224].
[26] D. Adams *et al.* [Spin Muon Collaboration (SMC)], Phys. Rev. D **56**, 5330 (1997) [arXiv:hep-ex/9702005].
[27] S. L. Zhu, S. Puglia and M. J. Ramsey-Musolf, Phys. Rev. D **63**, 034002 (2001) [arXiv:hep-ph/0009159].